

Encodings of the weighted MAX k -CUT on qubit systems

Franz G. Fuchs[†], Ruben P. Bassa[†], and Frida Lien[‡]

[†]SINTEF AS, Department of Mathematics and Cybernetics, Oslo, Norway

[‡]University of Oslo, Department of Mathematics, Oslo, Norway

December 1, 2024

Abstract

The weighted MAX k -CUT problem involves partitioning a weighted undirected graph into k subsets to maximize the sum of the weights of edges between vertices in different subsets. This problem has significant applications across multiple domains. This paper explores encoding methods for MAX k -CUT on qubit systems, utilizing quantum approximate optimization algorithms (QAOA) and addressing the challenge of encoding integer values on quantum devices with binary variables. We examine various encoding schemes and evaluate the efficiency of these approaches. The paper presents a systematic and resource efficient method to implement phase separation for diagonal square binary matrices. When encoding the problem into the full Hilbert space, we show the importance of balancing the “bin sizes”. We also explore the option to encode the problem into a suitable subspace, by designing suitable state preparations and constrained mixers (LX- and Grover-mixer). Numerical simulations on weighted and unweighted graph instances demonstrate the effectiveness of these encoding schemes, particularly in optimizing circuit depth, approximation ratios, and computational efficiency.

1 Introduction and related work

The quantum approximate optimization algorithm [5]/quantum alternating operator ansatz [11] (QAOA) is a widely studied hybrid algorithm for approximately solving combinatorial optimization problems encoded into the ground state of a Hamiltonian. Given an objective function $f : \{0, 1\}^n \rightarrow \mathbb{R}$, the problem Hamiltonian is defined as $H_P |x\rangle = f(x) |x\rangle$. Thus, the ground states of H_P correspond to the minima of the objective function. In the general framework of QAOA, a parameterized quantum state is prepared as follows:

$$|\gamma, \beta\rangle = U_M(\beta_p) U_P(\gamma_p) \cdots U_M(\beta_1) U_P(\gamma_1) |\phi_0\rangle. \quad (1)$$

Starting from an initial state $|\phi_0\rangle$, the algorithm alternates between applying the phase-separation operator $U_P(\gamma)$ and the mixing operator $U_M(\beta)$. The goal is to optimize the parameters $\gamma, \beta \in \mathbb{R}$ such that $\langle \gamma, \beta | H_P | \gamma, \beta \rangle$ is minimized.

Since the original proposal of QAOA, several extensions and variants have been introduced. One such extension is ADAPT-QAOA [15], an iterative version that iteratively adds only the terms that contribute to lowering the expectation value the most. Another variant is R-QAOA [3], which progressively removes variables from the Hamiltonian until the reduced instance can be classically solvable. A third extension, WS-QAOA [4], incorporates solutions from classical algorithms to warm-start the QAOA process. When a given problem has constraints, the design of mixers is vital. For constrained problems, the design of mixers is crucial. A well-known example is the XY -mixer [12, 14], which restricts evolution to “ k -hot” states. GM-QAOA [2] uses Grover-like operators for all-to-all mixing of more general feasible subsets. The mixing operator of GM is comprised of a circuit U_S that prepares the uniform superposition of all feasible states, its inverse U_S^\dagger and a multi-controlled rotational phase shift gate. Inspired by the stabilizer formalism, the LX-Mixer [8, 9] is a generalization of the aforementioned methods that provides a flexible framework that allows for tailored mixing within the feasible subspace.

To increase the practical relevance of QAOA, encoding problems with integer values, rather than binary variables, into qubit systems is an important research area. This process generally introduces considerable flexibility in encoding choices, affecting not only the number of qubits and controlled operations needed, but also the complexity of the optimization landscape and the quality of the approximation ratios that can be achieved. In this paper, we explore various encoding schemes for the MAX k -CUT problem into qubit systems, building on and improving earlier work [7]. This problem has numerous applications, including the placement of television commercials in program breaks, arrangement of containers on a ship with k bays, partition a set of items (e.g. books sold by an online shop) into k subsets, product module design, frequency assignment, scheduling, and pattern matching [1, 10]. Given a weighted undirected graph $G = (V, E)$, the MAX k -CUT problem consists of finding a maximum-weight k -cut. This involves partitioning the vertices into k subsets such that the sum of the weights of the edges between vertices in different

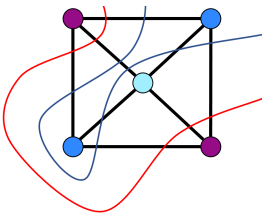


Figure 1: An example of an optimal solution for a MAX 3-CUT problem.

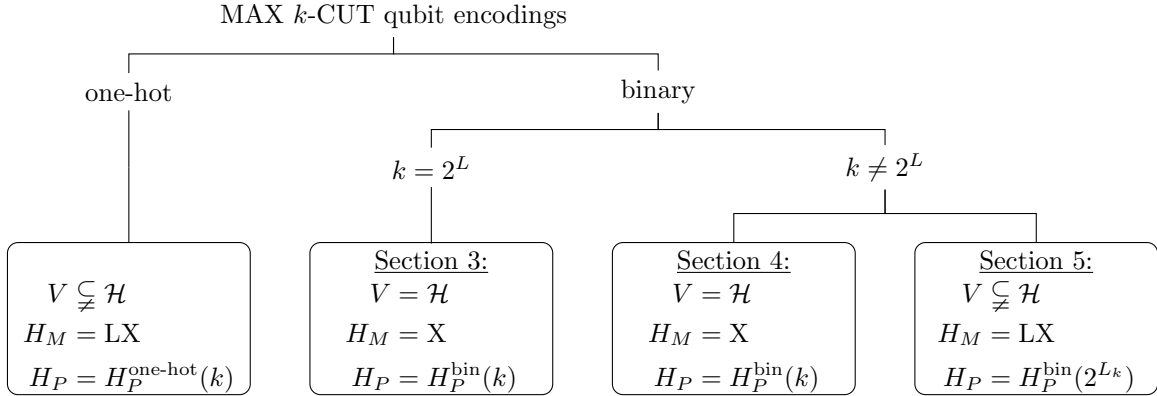


Figure 2: Overview of different ways to encode the problem.

subsets is maximized, as illustrated in Figure 1. By assigning a label $x_i \in \{1, \dots, k\}$ to each vertex $i \in V$ and defining $\mathbf{x} = (x_1, \dots, x_{|V|})$, the optimization problem for MAX k -CUT can be formulated as

$$\max_{\mathbf{x} \in \{1, \dots, k\}^n} C(\mathbf{x}), \quad C(\mathbf{x}) = \sum_{(i,j) \in E} \begin{cases} w_{ij}, & \text{if } x_i \neq x_j \\ 0, & \text{otherwise.} \end{cases} \quad (2)$$

Here, $w_{ij} > 0$ is the weight of edge $(i, j) \in E$. The function $C(\mathbf{x})$ is commonly referred to as the cost function. For $k = 2$ the MAX k -CUT problem becomes the well known MAX CUT problem. The MAX k -CUT problem is NP-complete, and it has been demonstrated that no polynomial-time approximation scheme exists for $k \geq 2$, unless P=NP [6].

A randomized approximation algorithm for (2) has an approximation ratio α if

$$\mathbb{E}[C(\mathbf{x})] \geq \alpha C(\mathbf{x}^*), \quad (3)$$

where \mathbf{x}^* denotes an optimal solution.

Expressing the solutions as strings of k -dits as in Equation (2) is a natural extension of the MAX (2-)CUT problem to $k > 2$. However, most quantum devices work with a two-level system, so we need to make a suitable encoding on qubits system [7, 11]. *One-hot encoding* uses k bits for each vertex, where the single bit that is 1 encodes which set/color the vertex belongs to. Using this encoding requires $k|V|$ qubits. However, when k is not a power of two, this results in more computational states per vertex than there are colors. The corresponding subspaces need to be dealt with in a suitable fashion. The Grover or the LX-mixer (which becomes the XY-mixer in this case) can be readily applied. However, the ratio of the dimension of the feasible states to the system size is $k/2^k$ which becomes exponentially small for increasing k . Therefore, it is advantageous to use a *binary encoding*, which does not have this problem. For a given k we encode the information of a vertex belonging to one of the sets by $|i\rangle_{L_k}$, which requires

$$L_k := \lceil \log_2(k) \rceil \quad (4)$$

qubits. Here $\lceil \cdot \rceil$ means rounding up to the nearest integer. Binary encoding requires $L_k|V|$ qubits, i.e., exponentially fewer qubits as compared to one-hot encoding. The resulting problem Hamiltonian can be written as the sum of local terms, i.e.,

$$H_P = \sum_{e \in E} w_e H_e, \quad (5)$$

where $w_{i,j}$ is the weight of the edge between vertices i and j . Furthermore, the local term can be expressed as

$$H_e = 2\widehat{H}_e - I, \quad \widehat{H}_e = \sum_{i,j=1}^{2^{L_k}} |i\rangle \langle i| \otimes |j\rangle \langle j|. = \sum_{(i,j) \in \text{clr}} |i\rangle \langle i| \otimes |j\rangle \langle j|. \quad (6)$$

Here, \sim_{clr} is an equivalence relation on the set $\{0, 2^{L_k} - 1\}$ given by a relation $\text{clr} = \{\text{sets of equivalent colors}\}$. With this, it is clear that $H_{i,j}$ has eigenvalue +1 for a state $|i\rangle |j\rangle$ if $i \sim_{\text{clr}} j$ and -1 if not. The phase separating operator e^{-itH_e} is equal to $e^{-it\widehat{H}_e}$ up to a scaling factor and a global phase, which will be used throughout the paper.

An overview of possible encoding techniques is provided in Figure 2. When k is not a power of two, we have to deal with the fact that we have non-trivial equivalence classes clr . There are two ways to deal with this. The first is to directly implement the phase separating Hamiltonian on the full Hilbert space [7], or to restrict the evolution onto the relevant subspace. The main contributions of this article are for the cases when k is not a power of two.

- We introduce a systematic way to implement the phase separating Hamiltonian, resulting in a reduction of the complexity of the resulting circuit, see Section 2.

- A method to directly work with a feasible subspace with a suitable state preparation and constrained mixer, see Section 5.
- More balanced sets of equivalent colors, which help to improve the resulting cost landscape, see Section 4.

We also employ the Grover mixer to all cases, indicating that the resulting landscape might be favourable. Throughout the paper the notation $C^l U$ means an l -controlled U gate. E.g., a Toffoli gate is $C^2 X$ and $CP = CP(\theta)$ is the controlled phase shift gate, where we mostly omit the parameter.

2 Realizing exponentials of diagonal matrices with binary elements

In this section we derive a general method to realize the exponential of a *diagonal square binary* matrix Λ , i.e.,

$$\Lambda_{i,j} \in \begin{cases} \{0, 1\}, & \text{if } i = j \\ \{0\}, & \text{otherwise,} \end{cases} \quad \forall 0 \leq i, j \leq 2^n - 1 \quad (7)$$

with quantum gates. If the number of non-zero elements is a power of two we have the following result.

Lemma 1

Let Λ be as in Equation (7), and r be the number of non-zero elements. Let $\mathcal{H} = A \otimes B$. If r is a power of two, then for any subsystem A of $\log(r)$ qubits and any computational basis state $|z\rangle_B$, there exists a permutation matrix P_π such that

$$e^{-i\theta\Lambda} = P_\pi (I_A \otimes D_z) P_\pi^{-1}, \quad D_z = I_B + (e^{-i\theta} - 1) |z\rangle_B \langle z|_B. \quad (8)$$

Moreover,

- P_π can be realized with gates from the set $\{X, CX, CCX\}$, and
- D_z resembles the well-known diffusion operators used in amplitude amplification and can be realized with a $n - \log(r) - 1$ controlled phase shift gate, sandwiched between X -gates on the wires where z is zero.

Proof. We start by observing that Λ is a projection, i.e., $\Lambda^2 = \Lambda$. Further, it makes sense to write the matrix $I_A \otimes |z\rangle_B \langle z|_B$, where A and B are qubit systems with $|A| = \log(r)$, and $|B| = n - |A|$. It is easy to convince yourself that the matrix $I_A \otimes |z\rangle_B \langle z|_B$ is a diagonal square binary matrix with the same number of non-zero elements as Λ . Hence, there exists a permutation P_π , such that $\Lambda = P_\pi (I_A \otimes |z\rangle_B \langle z|_B) P_\pi^{-1}$. From this it follows that

$$e^{-i\theta\Lambda} = \left(\sum_{l=0}^{\infty} \frac{(-i\theta)^l}{l!} \Lambda^l \right) = I + \left(\sum_{l=1}^{\infty} \frac{(-i\theta)^l}{l!} \Lambda \right) = I + (e^{-i\theta} - 1)\Lambda = P_\pi (I_A \otimes (I_B + (e^{-i\theta} - 1) |z\rangle_B \langle z|_B) P_\pi^{-1}. \quad (9)$$

Every permutation can be expressed as a product of transpositions (swaps of two elements). The X, CX, CCX gates allow us to implement these transpositions between specific pairs of basis states. By combining these gates in an appropriate sequence, we can generate any permutation matrix, as any such matrix corresponds to some sequence of swaps between basis states.

All elements of the diagonal matrix D_z are equal to one, except in the index $(\text{int}(z), \text{int}(z))$. Hence, D_z can be performed by a multi-controlled phase shift gate, modulo X gates. \square

Note that any n -qubit computational basis state transposition can be performed with $\Theta(n)$ gates, and there exists an explicit construction [13] of the circuit. In general, one needs $\mathcal{O}(r)$ transpositions, but in our cases we can realize P_π with $\mathcal{O}(n)$ gates from the set $\{X, CX, CCX\}$.

Theorem 1 (Realizing diagonal operators)

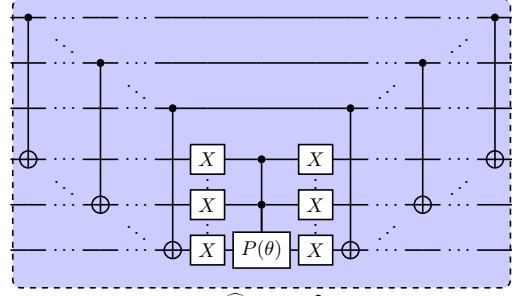
Let Λ be as in Equation (7) with r non-zero elements. We can always write r as a sum of powers of two, i.e., $r = 2^{q_1} + 2^{q_2} + \dots + 2^{q_p}$. The simplest way is use the binary representation of r , but using the same power multiple times is also allowed. Then, we can always realize the unitary evolution in the form

$$e^{-it\Lambda} = \hat{P}_{\pi_0} \prod_{j=1}^p \hat{D}_j \hat{P}_{\pi_j}, \quad (10)$$

where \hat{P}_{π_j} are permutation matrices that can be realized with gates from the set $\{X, CX, CCX\}$, and \hat{D}_j has the form $\hat{D}_j = I_{A_{q_j}} \otimes D_{z_{q_j}}$, where $D_{z_{q_j}}$ can be realized with an $(n - |A_{q_j}| - 1)$ -controlled shift gate.

	mixer	$k = 2$	$k = 4$	$k = 8$
Erdős- Rényi	X	0.87	0.89	0.97
	Grover \square	0.87	0.90	0.98
	Grover	0.79	0.83	0.93
Barabási- Albert	X	0.80	0.87	0.96
	Grover \square	0.80	0.88	0.96
	Grover	0.74	0.82	0.92

(a) Achieved approximation ratios.



(b) Circuit for realizing $e^{i\theta\hat{H}_e}$, for \hat{H}_e given in Equation (13).

Figure 3: Results for the case when $k = 2^{L_k}$.

Proof. Let $r = 2^{q_1} + 2^{q_2} + \dots + 2^{q_p}$. Then we can divide Λ into a sum of matrices with corresponding many non-zero elements, i.e.,

$$\Lambda = \Lambda_{q_1} + \Lambda_{q_2} + \dots + \Lambda_{q_p}. \quad (11)$$

For all matrices Λ_{q_i} in the above sum the number of non-zero elements is a power of two. Hence, we can apply Lemma 1, to get

$$e^{-i\theta\Gamma} = \prod_{j=1}^p e^{-i\theta\Gamma_j} = \prod_{j=1}^p P_{\pi_j} (I_{A_j} \otimes D_{z_j}) P_{\pi_j}^{-1}, \quad (12)$$

where the second equality holds, because diagonal matrices commute. Defining $\hat{P}_{\pi_0} = P_{\pi_1}$, $\hat{P}_{\pi_p} = P_{\pi_p}^{-1}$, and $\hat{P}_{\pi_j} = P_{\pi_{j-1}}^{-1} P_{\pi_j}$ for $1 \leq j \leq p-1$ proves the assertion. \square

Theorem 1 will be used in the following to create efficient quantum circuits for $k \in \{2, 3, \dots, 8\}$.

3 Binary encodings when k is a power of two

When $k = 2^{L_k}$ the equivalence relation for the problem Hamiltonian in Equation (6) becomes trivial, i.e., $\text{clr} = \{\{0, 0\}, \{1, 1\}, \dots, \{k-1, k-1\}\}$, and hence

$$\hat{H}_e = \sum_{i=0}^{k-1} |i\rangle \langle i| \otimes |i\rangle \langle i|. \quad (13)$$

Observe that \hat{H}_e is a diagonal square binary matrix. This means we can directly apply Theorem 1 to know that there exists a subsystem A of size L_k , such that $\hat{D} = I_A \otimes D_z$, and D_z can be realized with an $(L_k - 1)$ -controlled phase shift gate. More concretely, observe that

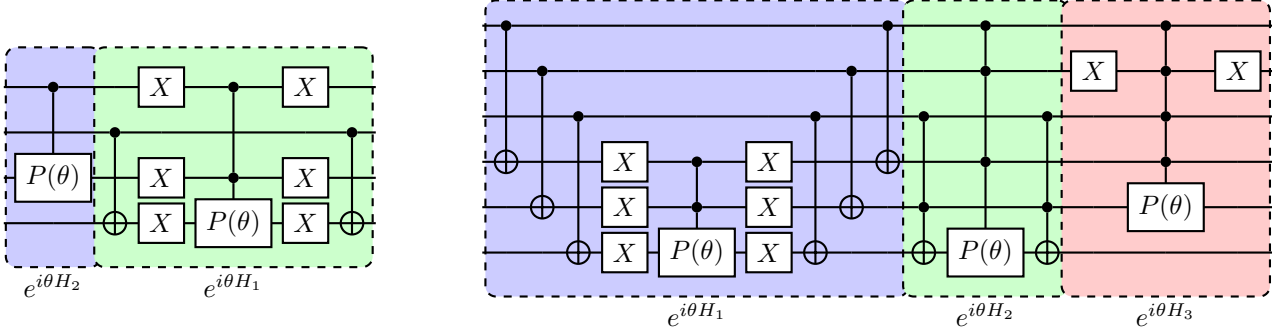
$$\hat{H}_e = CX_{A \rightarrow B} (I_A \otimes |0\rangle_B \langle 0|_B) CX_{A \rightarrow B}, \quad (14)$$

meaning that $|z\rangle_B = |0\rangle_B$. Here, $CX_{A \rightarrow B}$ is short hand for $CX_{A_1, B_1} CX_{A_2, B_2} \dots CX_{A_{L_k}, B_{L_k}}$. The resulting circuit is shown in Figure 3b.

Number of controlled gates for the mixer and phase separating operators.

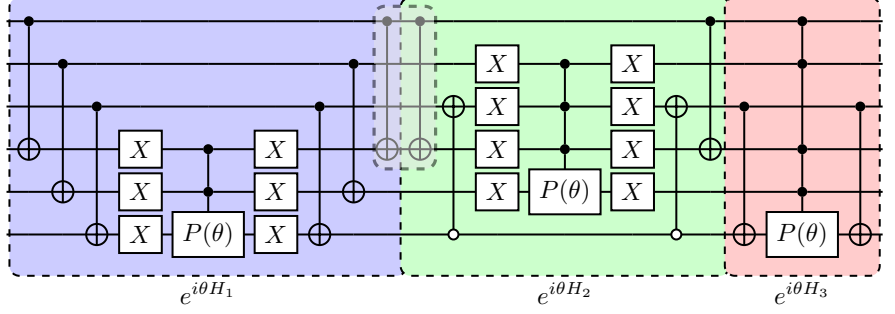
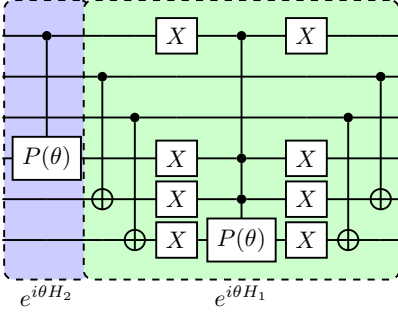
- Realizing $e^{-i\theta\hat{H}_e}$ through Equation (14) one needs $2L_k$ CX gates and 1 $C^{L_k-1}P$ gate. Alternatively, one can also do a direct decomposition of \hat{H}_e in the Pauli basis and perform Pauli evolution gates with this. For $k = 2, 4, 8$, the first approach needs $2CX$, ($4CX$ and $1CP$), and ($6CX$ and $1C^2P$), whereas the Pauli evolution needs $2CX$, $10CX$, $34CX$ per gate, respectively. Thus, for these cases it is better to realize the phase separation with the circuit given in Equation (14) and not through Pauli evolution.
- The X mixer does not require any controlled gates, the Grover mixer needs 1 $C^{|V|L_k-1}P$ gate, and the Grover \square^V needs $|V|$ $C^{L_k-1}P$ gates, where the box product is defined in Equation (37).

We numerically test the performance of the resulting QAOA algorithm on the same instances as in [7], given in Appendix A. Table 3a shows that the achieved approximation ratios are very good, for all cases. An overview of the energy/approximation ratio landscapes are provided in the Appendix in Table 2.



(a) $H_{\text{clr}_{<3}^3} = H_1 + H_2$ as defined in Equations (15) and (16).

(b) $H_{\text{clr}_{<6}^6} = H_1 + H_2 + H_3$ as defined in Equations (22) - (24).



(c) $H_{\text{clr}_{<5}^5} = H_1 + H_2$ as defined in Equations (17) and (18).

(d) $H_{\text{clr}_{\text{bal}}^5} = H_1 + H_2 + H_3$ as defined in Equations (13), (19) and (20). The gates in the gray box cancel to the identity. Note that $H_{\text{clr}_{\text{bal}}^6} = H_1 + H_2$.

Figure 4: Realizations of the phase separating operator. For the case $k = 5$, two different equivalence relations are shown.

4 Binary encodings for $k \neq 2^{L_k}$ using the full Hilbert space

When k is not a power of two, the equivalence relation for the problem Hamiltonian in Equation (6) becomes non-trivial. One way to deal with this is what we will refer to as the $\leq k$ -encoding where we encode the color k into all states with $|i\rangle$ for $k \leq i \leq 2^{L_k} - 1$. This means we have $\text{clr}_{<k}^k = \{\{0, 0\}, \{1, 1\}, \dots, \{k-2, k-2\}\} \cup_{i,j=k-1}^{2^{L_k}-1} \{i, j\}$. Of course, this is not a unique choice, and one can come up with ways to “balanced” the size of the bins for all colors, which we will denote as $\text{clr}_{\text{bal}}^k$. This also influences the resulting number of ones in the Hamiltonian \widehat{H}_e . In the following, we will make a concrete construction of the Hamiltonians for $k \in \{3, 5, 6, 7\}$.

4.1 The case $k = 3$

For $\text{clr}_{<3}^3$ the number of ones in \widehat{H}_e is equal to 6. According to Theorem 1 with $6 = 2^2 + 2^1$, this means we can realize the phase separating unitary with a one single and one double controlled phase shift gate. The +1 eigenstates of the Hamiltonian are $|0000\rangle, |0101\rangle, |1010\rangle, |1111\rangle, |1011\rangle, |1110\rangle$, where the first three states belong to three different color sets, and the last three to the remaining one. Dividing $\widehat{H}_e = H_1 + H_2$ it is easy to check that

$$H_1 = \sum_{(i,j) \in \text{clr}_{<3}^3, |i,j| \leq 1} |ij\rangle \langle ij| = CX_{2,4} (|0\rangle \langle 0| \otimes I \otimes |0\rangle \langle 0| \otimes |0\rangle \langle 0|) CX_{2,4}, \quad (15)$$

$$H_2 = \sum_{(i,j) \in \text{clr}_{<3}^3, |i,j| \geq 2} |ij\rangle \langle ij| = |1\rangle \langle 1| \otimes I \otimes |1\rangle \langle 1| \otimes I, \quad (16)$$

where $CX_{a,b}$ denotes a CX gate with control index a and target index b . The resulting circuit is show in Figure 4a. For $k = 3$ there is no way to balance the size of the bins more.

4.2 The case $k = 5$

For $\text{clr}_{<5}^5$ the number of ones in \widehat{H}_e is equal to 20. According to Theorem 1 with $20 = 2^4 + 2^2$, this means we can realize the phase separating unitary with a one single and one triple controlled phase shift gate. Dividing $\widehat{H}_e = H_1 + H_2$ it

is easy to check that

$$H_1 = \sum_{(i,j) \in \text{clr}_{<5}^5 |i,j \leq 3} |ij\rangle \langle ij| = CX_{1,4} CX_{2,5} \left(I_{1,2} \otimes |0\rangle \langle 0|_{0,3,4,5} \right) CX_{1,4} CX_{2,5}, \quad (17)$$

$$H_2 = \sum_{(i,j) \in \text{clr}_{<5}^5 |i,j \geq 4} |ij\rangle \langle ij| = I_{1,2,4,5} \otimes |1\rangle \langle 1|_{0,3}, \quad (18)$$

where the indices of $|\cdot\rangle \langle \cdot|$ and I indicate the indices of the qubits. The resulting circuit is show in Figure 4. Looking at the case for $k = 3$ and $k = 5$ it becomes clear that the circuit is generalizable for $\tilde{k} = 2^l + 1$: The number of ones for $\text{clr}_{<\tilde{k}}^{\tilde{k}}$ is equal to $2^{\tilde{k}-1} + 2^{\tilde{k}-2}$. with one single and one

A second possibility is to encode the problem with as equal sized "bins" as possible. One example is given by $\text{clr}_{\text{bal}}^5 = \{\{0,0\}, \{1,1\}, \dots, \{7,7\}\} \cup \{\{0,1\}, \{1,0\}, \{4,5\}, \{5,4\}\} \cup \{\{6,7\}, \{7,6\}\}$. Dividing accordingly $\widehat{H}_e = H_1 + H_2 + H_3$, which has 14 nonzero elements, we know that H_1 has the form of Equation (13), and it is easy to check that

$$H_2 = \sum_{(i,j) \in \{\{0,1\}, \{1,0\}, \{4,5\}, \{5,4\}\}} |ij\rangle \langle ij| = CX_{0,3} C^0 X_{5,2} \left(I_{0,5} \otimes |0\rangle \langle 0|_{1,2,3,4} \right) CX_{0,3} C^0 X_{5,2}, \quad (19)$$

$$H_3 = \sum_{(i,j) \in \{\{6,7\}, \{7,6\}\}} |ij\rangle \langle ij| = CX_{2,5} \left(I_2 \otimes |1\rangle \langle 1|_{0,1,3,4,5} \right) CX_{2,5}, \quad (20)$$

$$(21)$$

4.3 The case $k = 6$

For $\text{clr}_{<6}^6$ the number of ones in \widehat{H}_e is equal to 14. According to Theorem 1 with $14 = 2^3 + 2^2 + 2^1$, this means we can realize the phase separating unitary with one 2-, one 3-, and one 4-controlled phase shift gate. Dividing $\widehat{H}_e = H_1 + H_2 + H_3$ it is easy to check that

$$H_1 = \sum_{(i,j) \in \text{clr}_{<7}^7 |i=j} |ij\rangle \langle ij| = CX_{1,2,3 \rightarrow 4,5,6} \left(I_{1,2,3} \otimes |0\rangle \langle 0|_{4,5,6} \right) CX_{1,2,3 \rightarrow 4,5,6}, \quad (22)$$

$$H_2 = \sum_{i \in \{7,8\}, i \neq j \geq 6} |ij\rangle \langle ij| = CCX_{2,4 \rightarrow 5} \left(I_{2,4} \otimes |1\rangle \langle 1|_{0,1,3,5} \right) CCX_{2,4 \rightarrow 5}, \quad (23)$$

$$H_3 = \sum_{i=6, j \in \{7,8\}} |ij\rangle \langle ij| = I_7 \otimes |1\rangle \langle 1|_{0,2,3,4} \otimes |0\rangle \langle 0|_1, \quad (24)$$

where CCX is the Toffoli gate. The resulting circuit is show in Figure 4b.

A second possibility is to encode the problem with as equal sized "bins" as possible. One example is given by $\text{clr}_{\text{bal}}^6 = \{\{0,0\}, \{1,1\}, \dots, \{7,7\}\} \cup \{\{0,1\}, \{1,0\}, \{4,5\}, \{5,4\}\}$. Since $\text{clr}_{\text{bal}}^6 \cup \{\{6,7\}, \{7,6\}\} = \text{clr}_{\text{bal}}^5$ we can divide $\widehat{H}_e = H_1 + H_2$, with H_1 as in Equation (13) and H_2 as in Equation (19). The resulting circuit is shown in Figure 4d where the circuit for H_3 is dropped altogether.

4.4 The case $k = 7$

For $\text{clr}_{<7}^7$ the number of ones in \widehat{H}_e is equal to 10. According to Theorem 1 with $10 = 2^3 + 2^1$, this means we can realize the phase separating unitary with a one double and one 4-controlled phase shift gate. Dividing $\widehat{H}_e = H_1 + H_2$ it is easy to check that

$$H_1 = \sum_{(i,j) \in \text{clr}_{<7}^7 |i,j \leq 1} |ij\rangle \langle ij| = CX_{1,2,3 \rightarrow 4,5,6} \left(I_{1,2,3} \otimes |0\rangle \langle 0|_{4,5,6} \right) CX_{1,2,3 \rightarrow 4,5,6}, \quad (25)$$

$$H_2 = \sum_{(i,j) \in \text{clr}_{<5}^5 |i,j \geq 2} |ij\rangle \langle ij| = CX_{1,2,3 \rightarrow 4,5,6} \left(I_2 \otimes |1\rangle \langle 1|_{0,1,5} \otimes |0\rangle \langle 0|_{3,4} \right) CX_{1,2,3 \rightarrow 4,5,6}. \quad (26)$$

$$(27)$$

The resulting circuit is show in Figure 5.

4.5 Resource analysis

When k is not a power of two, the method presented in [7, Section 3.2.2] is not optimal in terms of resource efficiency; for each edge of the graph, it requires the circuit shown in Figure 3b and $a(a-1)$ times the circuit shown in Figure 6b, where $a = 2^{L_k} - (k-1)$. Each of these individual circuits uses $4 C^{L_k} X$ -gates, one $C^2 P$ gate and requires the use of two ancillary qubits. Concretely, for each edge one needs 2, 12, 6, 2, 56, \dots of these circuits for $k = 3, 5, 6, 7, 9, \dots$, respectively. The method derived from Theorem 1 on the other hand, requires much fewer entangling gates and does not require ancilla qubits. See Table 6a for a comparison.

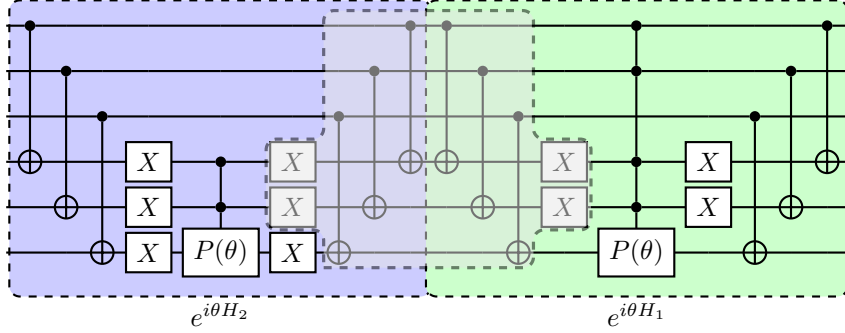
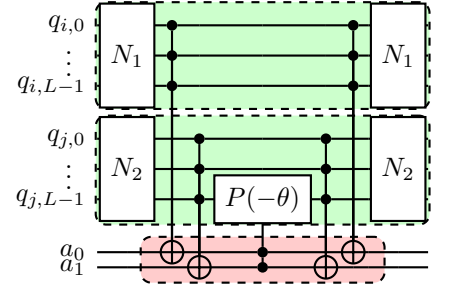


Figure 5: $H_{\text{chr}^7} = H_1 + H_2$ as defined in Equations (25) and (26). Note that $CX_{A \rightarrow B}$ and some of the X -gates of H_1 and H_2 cancel in the middle, marked with a gray shape.

k	[7, Section 3.2.2]	this work
3	$1CP, 2(4C^2X, 1C^2P), 4CX$	$1CP, 1C^2P, 2CX$
5	$1C^2P, 12(4C^3X, 1C^2P), 6CX$	$1CP, 1C^3P, 4CX$
6	$1C^2P, 6(4C^3X, 1C^2P), 6CX$	$1C^2P, 1C^3P, 8CX$
7	$1C^2P, 2(4C^3X, 1C^2P), 6CX$	$1C^2P, 1C^3P, 2C^2X, 6CX$



(a) Number of controlled gates to realize the phase gate for one edge of the graph. (b) Phase gate required in previous work [7].

Figure 6: The resource comparison shows that the circuits for realizing the phase separating operator U_P as proposed in this work require fewer resources in terms of entangling gates as previous work [7]. Another advantage of the proposed method is that it does not require ancilla qubits. Whereas we realize the diagonal operator directly, previous work [7] utilized the circuit shown in (b) between each edge (i, j) . For each element in $\text{clr}^k \setminus \cup_{i,j} \{i, i\}$, one such circuit is necessary with $N_i = X^{\text{bin}(\cdot)}$.

5 Binary encodings for $k \neq 2^{L_k}$ using subspaces

When k is not a power of two, there is an alternative to encoding the problem in the full Hilbert space as presented in Section 4. Instead, one can restrict the evolution of the QAOA to a suitably chosen subspace spanned by a set B consisting of k computational basis states. Consequently, this means we need a way to prepare an initial state in a k -dimensional subspace for each vertex of the graph, and a mixer constrained to this subspace. We observe that

$$H_P^{\text{bin}}(2^{L_k}) \Big|_{\text{span}(B)} = H_P^{\text{bin}}(k), \quad (28)$$

which means we can use the circuit for the power of two case. Overall, this approach shifts complexity from the phase separating Hamiltonian to the mixer.

5.1 Initial state

For the MAX k -CUT problem, one possibility is to define the subspace for each vertex through $B_k = \{|i\rangle \mid 0 \leq i \leq k-1\}$. Since the feasible bit-strings admit a Cartesian product structure, the feasible subspace becomes a tensor product of the form

$$B_k^1 \otimes \cdots \otimes B_k^{|V|}. \quad (29)$$

An initial state can be prepared as the uniform superposition of all feasible basis states, i.e.,

$$|\Phi_0^{\leq k}\rangle^{\otimes |V|}, \quad \text{where } |\Phi_0^{\leq k}\rangle = \frac{1}{k} \sum_{i=0}^{k-1} |i\rangle. \quad (30)$$

One way to realize the initial state for $k \in 3, 5, 6, 7$ is shown in Figure 7.

5.2 Constrained Mixer

Given a feasible subspace $\text{span}(B) \subset \mathcal{H}$ a mixer U_M is then called valid [11] if it *preserves the feasible subspace*, i.e.,

$$U_M(\beta) |v\rangle \in \text{span}(B), \quad \forall |v\rangle \in \text{span}(B), \forall \beta \in \mathbb{R}, \quad (31)$$

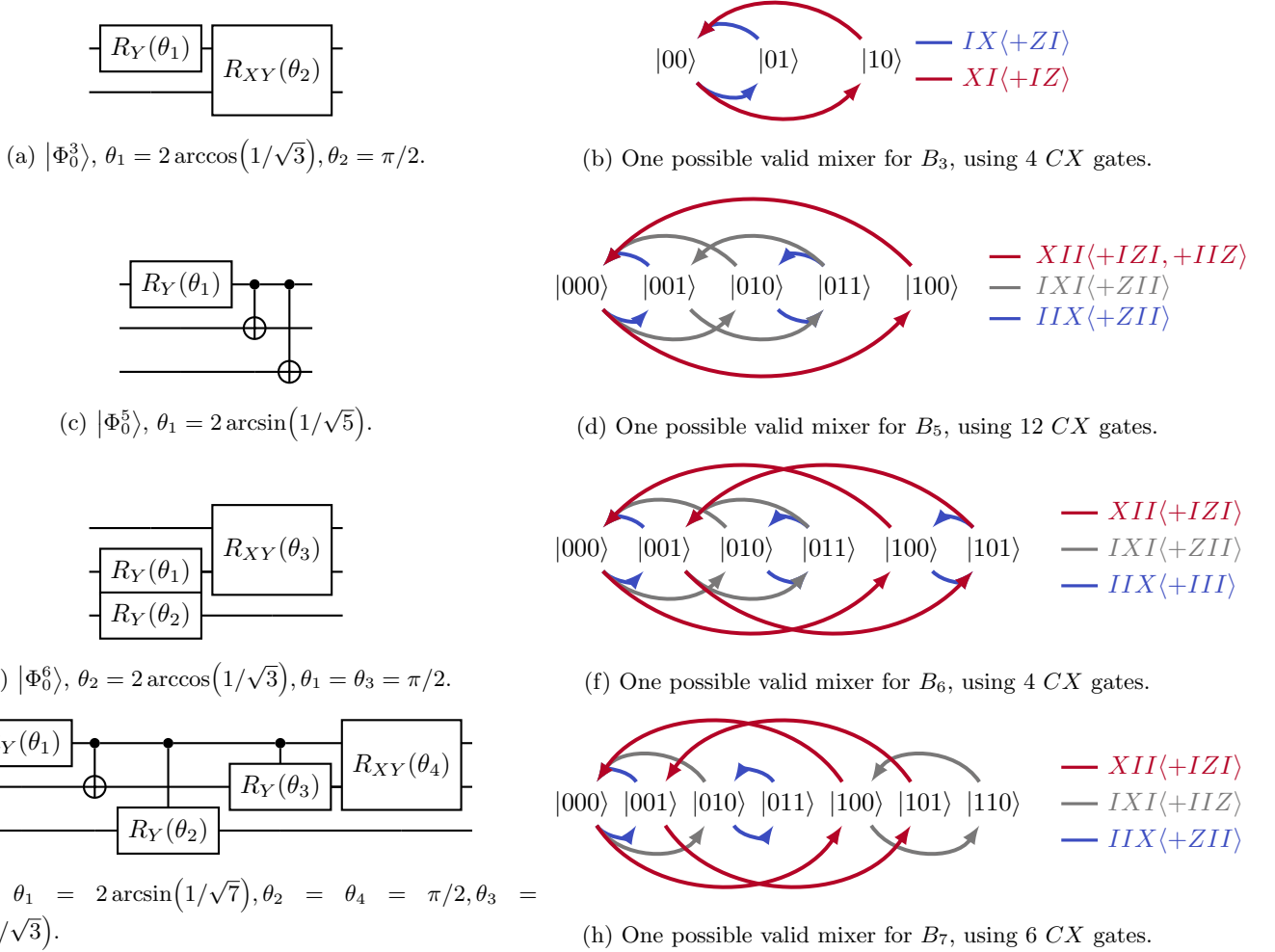


Figure 7: Initial state preparation and mixer for $k = 3, 5, 6, 7$ when restricting to a suitably chosen subspace. We use the notation $R_P(\theta) = \exp(-i\frac{\theta}{2}P)$, $P \in \{X, Y, Z\}$, and $R_{XY}(\theta) = \exp(-i\frac{\theta}{4}(X \otimes X + Y \otimes Y))$.

and if it provides transitions between all pairs of feasible states, i.e., for each pair of computational basis states $|x\rangle, |y\rangle \in B$ there exist $\beta^* \in \mathbb{R}$ and $r \in \mathbb{N} \cup \{0\}$, such that

$$|\langle x | U_M^r(\beta^*) | y \rangle| > 0. \quad (32)$$

Apart from the Grover mixer, we consider here constraint preserving mixers in the stabilizer form [8], in which case the Hamiltonian can be written as

$$H_M = \sum_{\alpha} c_{\alpha} \bar{X}^{\alpha} \prod_{V_{\alpha}}, \quad (33)$$

where $\alpha \in \{0, 1\}^n \setminus \{0\}^n$ is a multi-index, $\bar{X}^{\alpha} = X_1^{\alpha_1} \cdots X_n^{\alpha_n} \in \{I, X\}^n \setminus \{I\}^n$, and $\prod_{V_{\alpha}}$ is a projection onto V_{α} . Furthermore, V_{α} is a subspace fulfilling $|x\rangle \in V_{\alpha} \Rightarrow \bar{X}^{\alpha} |x\rangle \in V_{\alpha}$. The free parameter $c_{\alpha} \in \{0, 1\}$ must be chosen such that we have a valid mixer. Let $\{S_1, \dots, S_l\}$ be a minimal generating set of the stabilizer group $S = \langle S_1, \dots, S_l \rangle$ defining the code subspace $C(S)$. We can choose the projection operator to be of the form

$$\prod_{C(S)} = \frac{1}{2^k} \sum_{S \in \langle S_1, \dots, S_k \rangle} S. \quad (34)$$

For more details we refer the reader to [8]. In the following, we will use the notation

$$\bar{X} \langle S_1, \dots, S_k \rangle := \frac{1}{2^k} \sum_{S \in \langle S_1, \dots, S_k \rangle} \bar{X} S. \quad (35)$$

Given the independence of the different color constraints for each vertex of the problem, we can then define the following LX-mixer Hamiltonian

$$H_M = G^{\square^{|V|}} = G \square G \cdots \square G, \quad (36)$$

where the Cartesian or Box product is defined as

$$G \square H = G \otimes \mathbb{I} + \mathbb{I} \otimes H. \quad (37)$$

	mixer	$ \phi_0\rangle$	clr	$k = 3$	$k = 5$	$k = 6$	$k = 7$
Erdős-Rényi	X	$ +\rangle$	$\text{clr}_{<k}^k$	0.80	0.86	0.92	0.95
	X	$ +\rangle$	$\text{clr}_{\text{bal}}^k$	-	0.90	0.94	-
	LX	$ \Phi_0^{<k}\rangle$	-	0.80	0.91	0.94	0.94
	Grover \square	$ \Phi_0^{<k}\rangle$	-	0.83	0.94	0.96	0.97
	Grover	$ \Phi_0^{<k}\rangle$	-	0.75	0.87	0.90	0.92
Barabási-Albert	X	$ +\rangle$	$\text{clr}_{<k}^k$	0.79	0.84	0.90	0.93
	X	$ +\rangle$	$\text{clr}_{\text{bal}}^k$	-	0.88	0.92	-
	LX	$ \Phi_0^{<k}\rangle$	-	0.79	0.89	0.93	0.93
	Grover \square	$ \Phi_0^{<k}\rangle$	-	0.82	0.92	0.94	0.95
	Grover	$ \Phi_0^{<k}\rangle$	-	0.75	0.86	0.89	0.91

(a) Approximation ratios achieved for the graphs shown in Appendix A.

			$k = 3$	$k = 5$	$k = 6$	$k = 7$
X	$ +\rangle$	$H_P^{<k,\text{old}}(k)$	$70 E $	$782 E $	$398 E $	$142 E $
X	$ +\rangle$	$H_P^{<k,\text{Pauli}}(k)$	$18 E $	$66 E $	$258 E $	$130 E $
X	$ +\rangle$	$H_P^{<k}(k)$	$12 E $	$26 E $	$90 E $	$58 E $
X	$ +\rangle$	$H_P^{\text{bal,old}}(k)$	-	$398 E $	$270 E $	-
X	$ +\rangle$	$H_P^{\text{bal,Pauli}}(k)$	-	$130 E $	$66 E $	-
X	$ +\rangle$	$H_P^{\text{bal}}(k)$	-	$82 E $	$36 E $	-
LX	$ \Phi_0^{<k}\rangle$	$H_P(2^{L_k})$	$(2+4) V + 6 E $	$(2+12) V + 14 E $	$(2+4) V + 14 E $	$(5+6) V + 14 E $
Grover \square	$ \Phi_0^{<k}\rangle$	$H_P(2^{L_k})$	$(2+6) V + 6 E $	$(2+12) V + 14 E $	$(2+12) V + 14 E $	$(5+18) V + 14 E $

(b) Cost in terms of CX gates, when using the qiskit compiler. Methods from previous work is marked with light gray background: The line with $H_P^{\text{old}}(k)$ is the Hamiltonian presented in [7], and the $H_P^{\text{Pauli}}(k)$ decomposes the Hamiltonian in the Pauli basis. Terms related to the phase separating Hamiltonian scale with the number of edges and terms related to the mixer scale with the number of vertices. Notice that by encoding the problem in a specific subspace, rather than the entire Hilbert space, the complexity is shifted away from the phase-separating Hamiltonian and instead transferred to the mixer.

Table 1: Comparison of different encoding schemes when k is not a power of two. The X-mixer uses the encoding of the full Hilbert space presented in Section 4, whereas the LX- and Grover mixers encode the problem in a subspace as described in Section 5.

It can be shown that if G is a valid mixer, so is H_M constructed in this way [8]. Valid mixers with optimal cost in terms of CX gates are shown in Figure 7 for $k \in \{3, 5, 6, 7\}$. We note, that this choice is not unique and other mixers are possible as well.

6 Simulations

We perform numerical simulations for an unweighted Erdős-Rényi graph and a weighted Barabási-Albert graph with 10 vertices, shown in Appendix A. Since the case when k is a power of two is presented in Section 3, we will focus here on evaluating the methods presented in Sections 4 and 5. Using an ideal simulator we compare the results for the binary encoding with the standard X-mixer and different choices of equivalence relations to encode the colors, and the subspace encoding with different choices of mixers. The resulting energy landscapes are provided in Appendix A. As expected, the landscapes are periodic in β when using the X- and Grover-mixer, whereas the landscape associated to the LX-mixer is not in general. The resulting approximation ratios are shown in Table 1a. Overall, the subspace-encoding using the Grover \square mixer achieves the highest values for these two graphs, although with only a small distance to the LX-mixer. We can also see, that the balancing the bin sizes for the different colors has a very positive effect on the approximation ratio, when using the full Hilbert space and the X-mixer. We would like to note, however, that one should make a careful consideration of the averaged achieved approximation ratio with respect to the required circuit depth. For the encoding in the full Hilbert space, one can use the X-mixer, but the the phase-separation operator requires a deeper circuit. For the encoding into a subspace, one can use the phase-separation operator for the power of two case (leading to a more shallow circuit), but the circuit for the constrained preserving mixer is deeper. An indication of the cost is given in Table 1b, where we used the compiler from qiskit, assuming full connectivity. Note that for a sparse graph $|E| = \mathcal{O}(|V|)$ and for a fully connected graph $|E| = \Theta(|V|^2)$. Therefore, for graphs with sufficient connectivity, the subspace encoding uses fewer resources than the encoding into the full Hilbert space.

7 Availability of Data and Code

All data, e.g., graphs, and the python/jupyter notebook source code of the MAX k -CUT-implementation using QAOA for reproducing the results obtained in this article are available at <https://github.com/OpenQuantumComputing/QAOA/>. The code has been thoroughly developed with unit tests.

8 Author contributions

Franz G. Fuchs formulated the concept, developed the methodology, wrote the software, made the formal analysis and investigation, wrote the article, made the visualizations. Ruben Pariente Bassa developed the methodology, wrote part of the software, made the analysis, contributed to the article. Frida Lien wrote part of the software, contributed to the article.

9 Acknowledgment

We would like to thank for funding of the work by the Research Council of Norway through project number 332023. The authors wish to thank Terje Nilsen at Kongsberg Discovery for the access to an H100 GPU for the simulations.

10 Conclusion

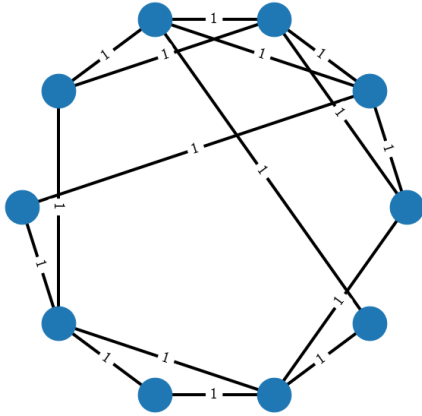
This study presents advancements in encoding the MAX k -CUT problem into qubit systems, with a focus on cases where k is not a power of two. We present new ways of encoding that significantly reduce the resource requirements compared to previous approaches. Balanced color sets and constrained mixers demonstrate notable improvements in optimization landscapes and approximation ratios. In the future we plan to do a careful analysis of which ansatz is preferable when k is not a power of two, using a suit of graph instances. The analysis should take into account the overall circuit depth, the achieved approximation ratio for increasing depth size, as well as if the landscape has barren plateaus or many “bad” local minima.

References

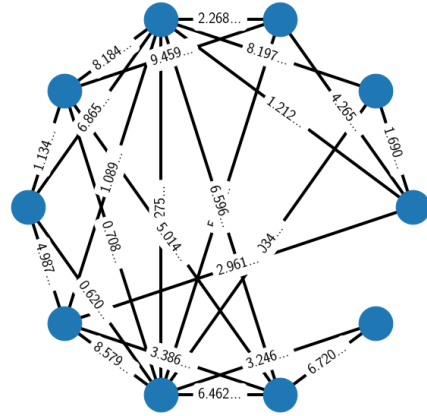
- [1] Karen I. Aardal et al. “Models and solution techniques for frequency assignment problems”. In: *Annals of Operations Research* 153.1 (May 2007), pp. 79–129. DOI: <https://doi.org/10.1007/s10479-007-0178-0>.
- [2] Andreas Bartschi and Stephan Eidenbenz. “Grover Mixers for QAOA: Shifting Complexity from Mixer Design to State Preparation”. In: *2020 IEEE International Conference on Quantum Computing and Engineering (QCE)*. IEEE, Oct. 2020. DOI: <https://doi.org/10.1109/qce49297.2020.00020>.
- [3] Sergey Bravyi et al. “Obstacles to variational quantum optimization from symmetry protection”. In: *Physical review letters* 125.26 (2020), p. 260505. DOI: <https://doi.org/10.1103/PhysRevLett.125.260505>.
- [4] Daniel J Egger, Jakub Mareček, and Stefan Woerner. “Warm-starting quantum optimization”. In: *Quantum* 5 (2021), p. 479. DOI: <https://doi.org/10.22331/q-2021-06-17-479>.
- [5] Edward Farhi, Jeffrey Goldstone, and Sam Gutmann. “A quantum approximate optimization algorithm”. In: *arXiv preprint arXiv:1411.4028* (2014). DOI: <https://doi.org/10.48550/arXiv.1411.4028>.
- [6] Alan Frieze and Mark Jerrum. “Improved approximation algorithms for maxk-cut and max bisection”. In: *Algorithmica* 18.1 (1997), pp. 67–81. DOI: <https://doi.org/10.1007/BF02523688>.
- [7] Franz G Fuchs et al. “Efficient encoding of the weighted max k-cut on a quantum computer using qaoa”. In: *SN Computer Science* 2.2 (2021), p. 89. DOI: <https://doi.org/10.1007/s42979-020-00437-z>.
- [8] Franz G. Fuchs and Ruben Pariente Bassa. “Optimal mixers restricted to subspaces and the stabilizer formalism”. In: *arXiv preprint arXiv:2306.17083* (2023). DOI: <https://doi.org/10.48550/ARXIV.2306.17083>.
- [9] Franz Georg Fuchs et al. “Constraint Preserving Mixers for the Quantum Approximate Optimization Algorithm”. In: *Algorithms* 15.6 (2022), p. 202. DOI: <https://doi.org/10.3390/a15060202>.
- [10] Daya Ram Gaur, Ramesh Krishnamurti, and Rajeev Kohli. “The capacitated max k-cut problem”. In: *Mathematical Programming* 115.1 (2008), pp. 65–72. DOI: <https://doi.org/10.1007/s10107-007-0139-z>.
- [11] Stuart Hadfield et al. “From the quantum approximate optimization algorithm to a quantum alternating operator ansatz”. In: *Algorithms* 12.2 (2019), p. 34. DOI: <https://doi.org/10.3390/a12020034>.
- [12] Stuart Hadfield et al. “Quantum approximate optimization with hard and soft constraints”. In: *Proceedings of the Second International Workshop on Post Moores Era Supercomputing*. 2017, pp. 15–21. DOI: <https://doi.org/10.1145/3149526.3149530>.

- [13] Steven Herbert, Julien Sorci, and Yao Tang. “Almost-optimal computational-basis-state transpositions”. In: *Physical Review A* 110.1 (2024), p. 012437. DOI: <https://doi.org/10.1103/PhysRevA.110.012437>.
- [14] Zihui Wang et al. “XY mixers: Analytical and numerical results for the quantum alternating operator ansatz”. In: *Physical Review A* 101.1 (Jan. 2020). DOI: <https://doi.org/10.1103/physreva.101.012320>.
- [15] Linghua Zhu et al. “Adaptive quantum approximate optimization algorithm for solving combinatorial problems on a quantum computer”. In: *Physical Review Research* 4.3 (2022), p. 033029. DOI: <https://doi.org/10.1103/PhysRevResearch.4.033029>.

A Graph instances



(a) Instance of the unweighted Erdős-Rényi graph.



(b) Instance of the weighted Barabási-Albert graph.

Figure 8: Graph instances used in this paper.

B Landscapes for the approximation ratio at $p = 1$

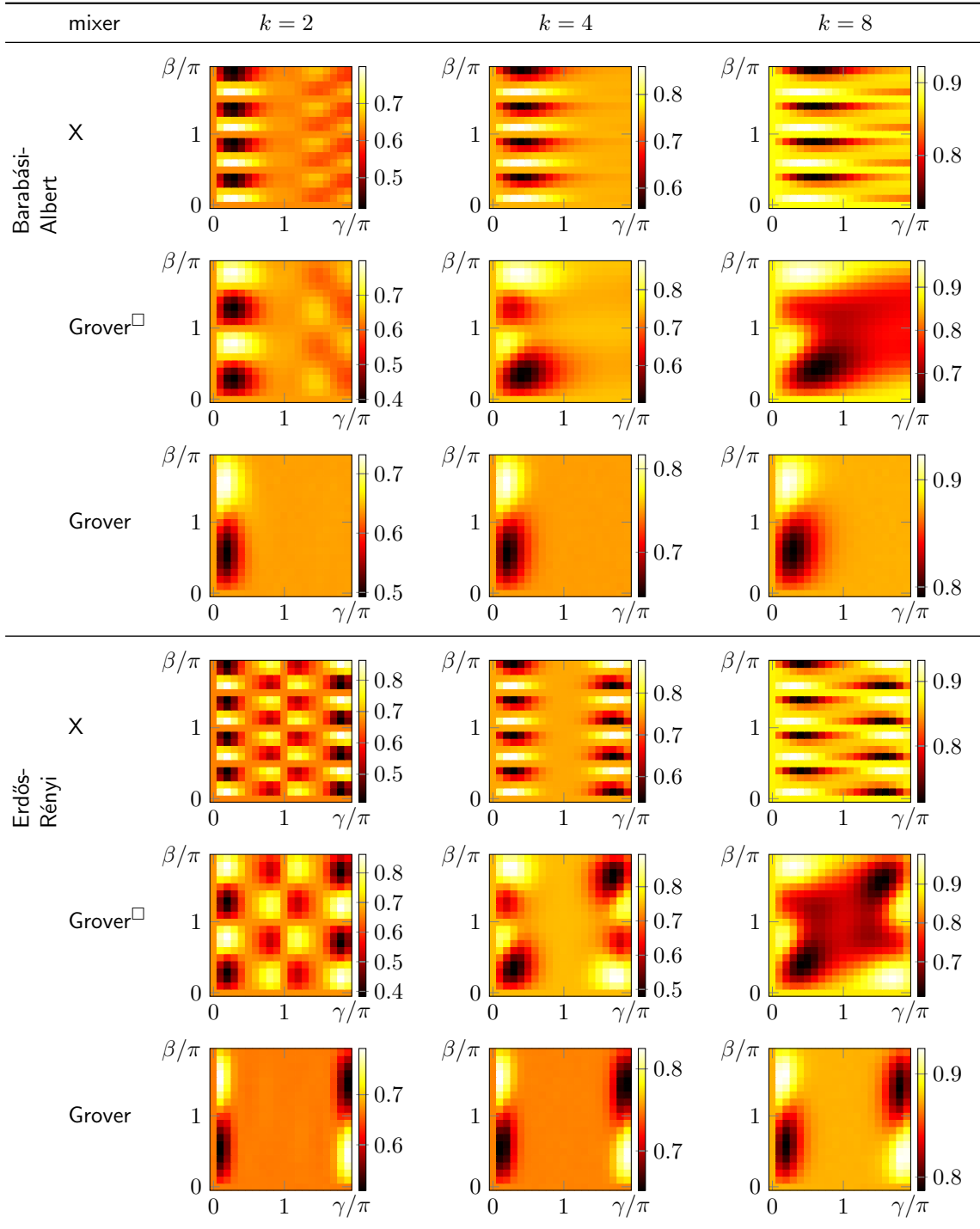


Table 2: Landscape of approximation ratios for depth $p = 1$ for the case when k is a power of two.

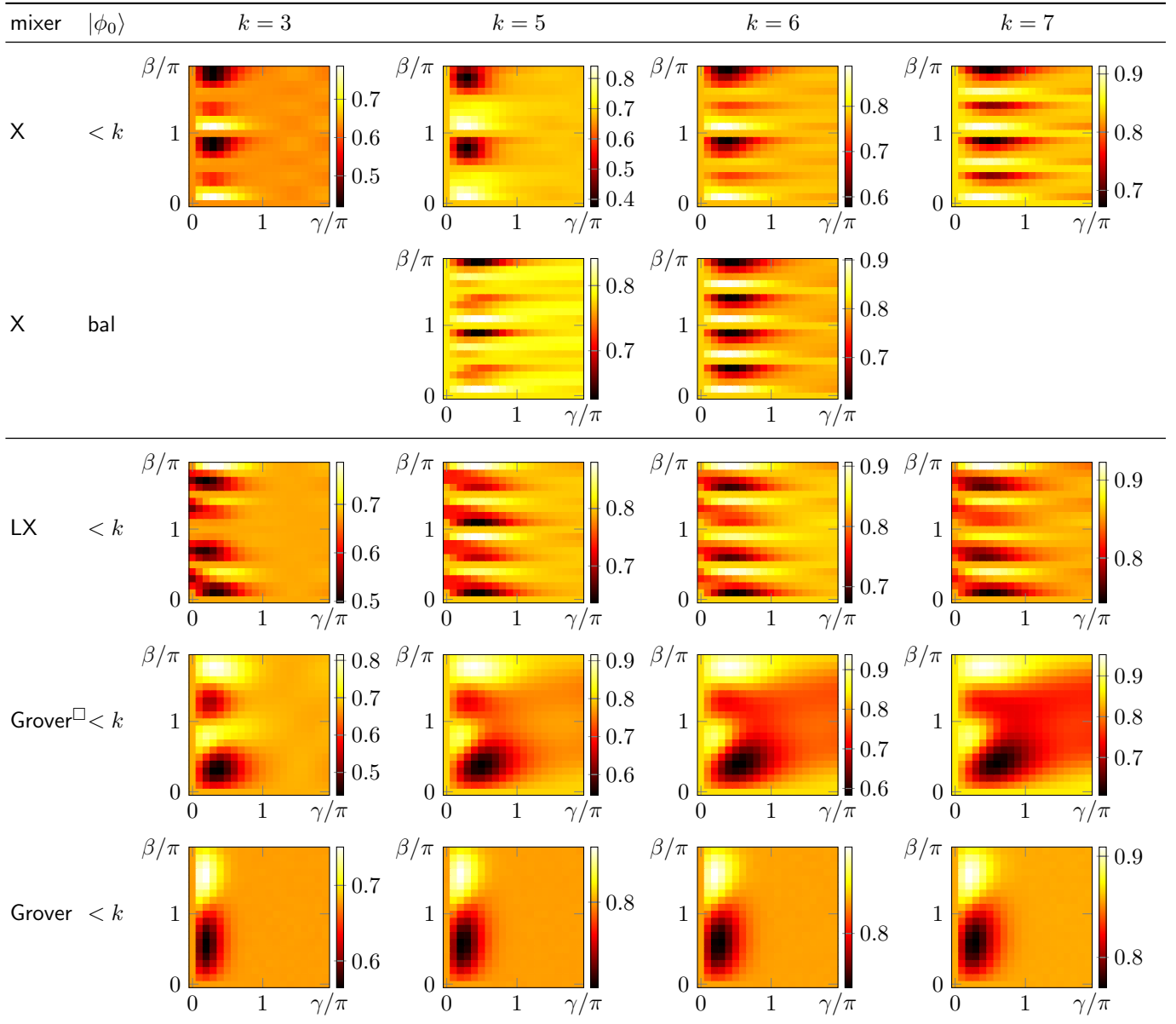


Table 3: Landscape of approximation ratios for depth $p = 1$ for the weighted Barabási-Albert graph.

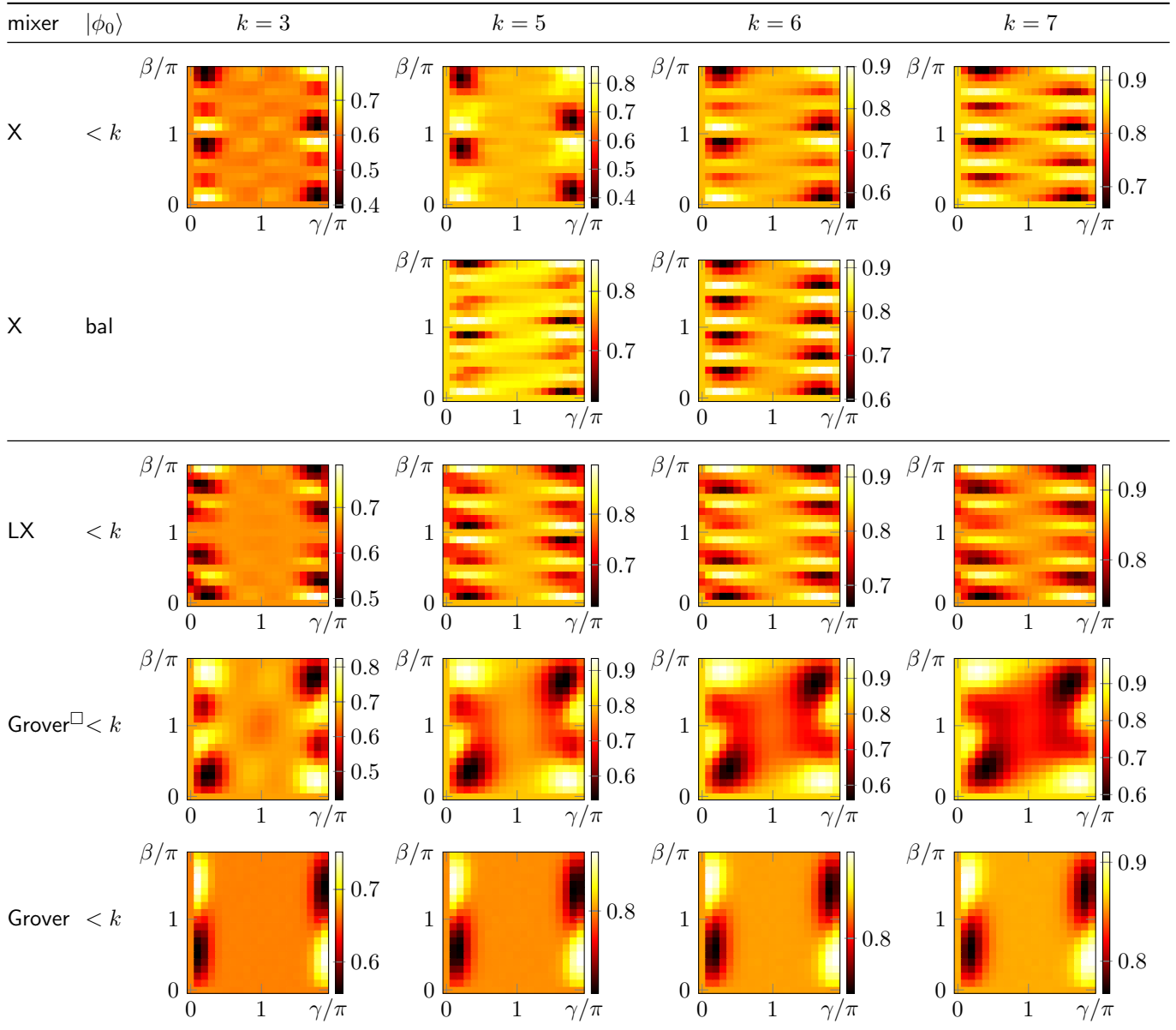


Table 4: Landscape of approximation ratios for depth $p = 1$ for the unweighted Erdős-Rényi graph.